ELSEVIER

Journal of Power Sources 68 (1997) 613–617

JOURNAL OF POWER SOURCES

Novel synthesis process and structure refinements of $Li_4Mn_5O_{12}$ for rechargeable lithium batteries

Toshimi Takada [a,*], Hiroshi Hayakawa [a], Etsuo Akiba [a], Fujio Izumi [b], Bryan C. Chakoumakos [c]

[a] National Institute of Materials and Chemical Research, Higashi 1-1, Tsukuba, Ibaraki 305, Japan
[b] National Institute for Research in Inorganic Materials, Namiki 1-1, Tsukuba, Ibaraki 305, Japan
[c] Oak Ridge National Laboratory, Oak Ridge, TN 37831-6393, USA

Accepted 14 October 1996

Abstract

Well-crystallized $Li_4Mn_5O_{12}$ powder with grain size of 0.1–0.4 μm was prepared by heating a eutectic mixture of lithium acetate (LiOAc), and manganese nitrate ($Mn(NO_3)_2$), in an oxygen atmosphere. The structure of $Li_4Mn_5O_{12}$ crystallites was found to be a cubic spinel using Rietveld refinement of both neutron and X-ray powder diffraction data. We confirmed that lithium ions occupy both the tetrahedral 8*a* sites, and part of the octahedral 16*d* sites, but not the 16*c* sites in the space group $Fd\bar{3}m$, while all the manganese ions occupy the 16*d* sites. The lattice parameter was found to be sensitive to the synthesis temperature as a result of the variation in manganese valence. Samples prepared at 500 °C showed better electrode performance. A rechargeable capacity of about 135 mAh/g for the cell $Li/Li_4Mn_5O_{12}$ was obtained in the 2.5–3.6 V range of cell voltages. © 1997 Elsevier Science S.A.

Keywords: Spinel; Structure refinement; Lithium manganese oxides; Rietveld method; Lithium batteries

1. Introduction

Extensive research has been directed toward the development and optimization of the lithium manganese oxide electrode for rechargeable lithium batteries. Particular attention has been given to the spinels $LiMn_2O_4$, $Li_4Mn_5O_{12}$ and $Li_2Mn_4O_9$ [1–7]. Currently, the spinel $Li[Li_xMn_{2-x}]O_4$ ($0.03<x<0.10$) is becoming more attractive because it shows better cycling performance. It is the current consensus that a wide range of solid solutions exists within the Li–Mn–O family of spinel compounds, and the composition of the spinel electrode plays a very important role in controlling the rechargeability of the electrode [3]. Therefore, attention should be paid to the control of the synthesis process to obtain single-phase samples with the required stoichiometry. Understanding the crystal structural changes during the synthesis process is crucial for both process control and understanding the variation of voltage, capacity, and cycling performance of Li/spinel cells.

In this study, we have focused on the synthesis process of well-crystallized $Li_4Mn_5O_{12}$, the confirmation of cation distribution by neutron diffraction, and structural changes caused by the presence of Mn^{3+}. The results of structure refinements by the Rietveld method using both X-ray and neutron powder diffraction data, and preliminary results of the electrode performance of $Li/Li_4Mn_5O_{12}$ are presented.

2. Experimental

2.1. Synthesis of $Li_4Mn_5O_{12}$

99.9% pure $LiOAc \cdot 2H_2O$ and $Mn(NO_3)_2 \cdot 6H_2O$ (from WAKO Pure Chemical Industries) were used as the starting materials. Stoichiometric amounts of the raw materials were first heated at 100 °C to obtain a uniform eutectic solution, and then slowly oxidized at 200 °C under flowing oxygen to convert the eutectic solution to a solid Li–Mn–O precursor. Powder samples were obtained by heating the ground precursor at a temperature ranging from 400 to 900 °C for 1 to 3 days. All samples were heated at a rate of 100 °C/h and slowly cooled to room temperature in the furnace (about 7 h) under flowing of oxygen (200 ml/min). Details of the preparation process were described in our previous report [4].

* Corresponding author

0378-7753/97/$17.00 © 1997 Elsevier Science S.A. All rights reserved
PII S0378-7753(96)02570-0

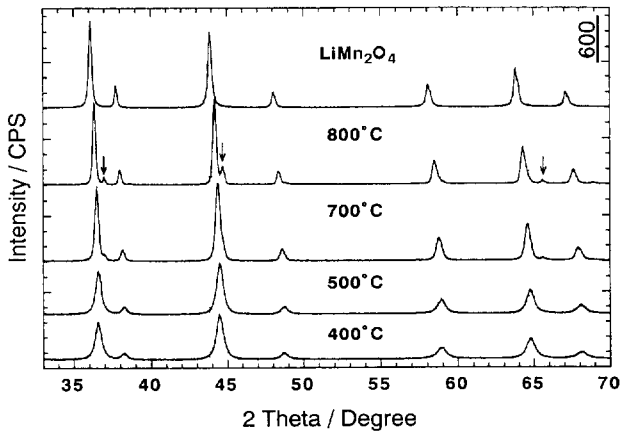

Fig. 1. X-ray diffraction patterns for $Li_4Mn_5O_{12}$ prepared at temperatures ranging from 400 to 800 °C under flowing oxygen using LiOAc and $Mn(NO_3)_2$ as the raw materials; for comparison those of $LiMn_2O_4$ is presented. Arrows indicate the reflections due to Li_2MnO_3.

2.2. X-ray diffraction

X-ray powder diffraction measurements were conducted at room temperature on a Rigaku RAX-I X-ray diffractometer with monochromatized Cu Kα radiation ($\lambda = 1.5406$ Å) at 40 kV and 30 mA. Data were collected between $2\theta = 15°$–120° with a step interval of 0.03°.

2.3. Neutron diffraction

Neutron diffraction data were collected using the HB4 high-resolution powder diffractometer at the High-Flux Isotope Reactor at Oak Ridge National Laboratory. The white beam of neutron from the reactor was monochromatized to a wavelength of 1.4180(2). The sample (about 4.5 g) was placed in a spinning vanadium can (internal diameter 1 cm, height 6 cm) during data collection over the 2θ range from 11° to 135° in steps of 0.05° at 295 K. Structural refinements were carried out with a Rietveld-refinement program, *RIETAN*-94 [8,9] for Power Macintosh.

2.4. Electrode performance

The electrode performance of $Li_4Mn_5O_{12}$ was examined in a conventional electrochemical cell at room temperature, using lithium metal as the negative and reference electrodes, and 1.0 M $LiPF_6$ dissolved in ethylene carbonate (EC) and dimethyl carbonate (DMC) (1:1 in volume) as the electrolyte. The composite electrode was made by mixing the $Li_4Mn_5O_{12}$ powder with 30.0 wt.% acetylene black and 4.0 wt.% of polyvinylidene fluoride (PVDF) dissolved in 1-methyl-2-pyrrolidone (NMP). The slurry was pressed onto an aluminum mesh current collector (10 mm × 10 mm).

3. Result and discussion

3.1. Synthesis of well-crystallized $Li_4Mn_5O_{12}$

Fig. 1 shows the powder X-ray diffraction patterns of $Li_4Mn_5O_{12}$ prepared at 400, 500, 700 and 800 °C from LiOAc + $Mn(NO_3)_2$, and for comparison, the $LiMn_2O_4$ standard. Clearly, higher reaction temperature gave sharper and higher diffraction peaks, and consequently a better crystallinity for $Li_4Mn_5O_{12}$. A minor monoclinic phase, Li_2MnO_3, however, appeared when the reaction temperature was raised above 700 °C. The reflections of Li_2MnO_3 in the sample obtained at 700 °C and below were negligible. All the visible reflections were consistent with those of the cubic spinel $LiMn_2O_4$, but with a visible shift to higher 2θ angles corresponding to the contraction of the unit cell from $a = 8.242$ Å for $LiMn_2O_4$ to $a = 8.1610(5)$ Å for $Li_4Mn_5O_{12}$.

Fig. 2 shows a typical scanning electron microscopy image of the $Li_4Mn_5O_{12}$ crystallites in the sample prepared at 700 °C. Micrographs (A) and (B) are for the sample prepared in powder form and in a pellet, respectively. Clearly, the size of $Li_4Mn_5O_{12}$ crystallites in these samples was uniformly distributed between 0.1–0.4 μm. Such uniformity in size and shape of the crystallites could be the result of the homogeneity of the Li–Mn–O precursor.

3.2. Structural refinement of $Li_4Mn_5O_{12}$ by the Rietveld method

The space group $Fd\bar{3}m$ was used for the structural refinement of $Li_4Mn_5O_{12}$, in combination with atomic coordinates obtained from our previous X-ray diffraction study [4]. The

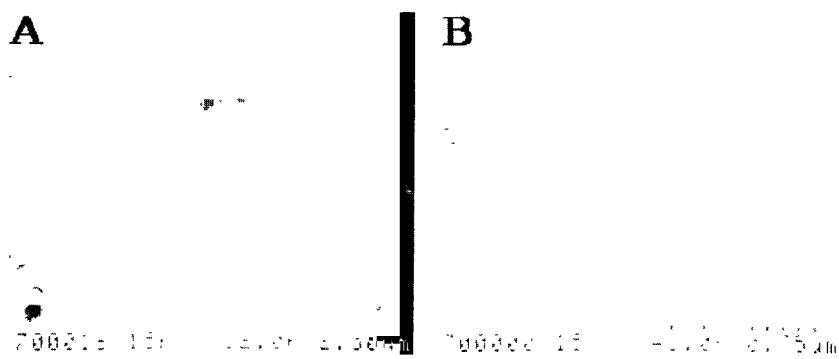

Fig. 2. Scanning electron micrographs of $Li_4Mn_5O_{12}$ crystallites in the sample prepared at 700 °C: (A) sample prepared in powder form, and (B) in a pellet, respectively.

following coherent scattering lengths were used: $b(\mathrm{Li}) = -0.1900\times10^{-14}$ m, $b(\mathrm{Mn}) = -0.3730\times10^{-14}$ m, $b(\mathrm{O}) = 0.5803\times10^{-14}$ m. The refinements included the two crystalline phases: $Li_4Mn_5O_{12}$ ($Fd\bar{3}m$, No. 227) and Li_2MnO_3 ($C/2m$, No. 12). The structural parameters of Strobel and Lambert-Andron [10] were used for Li_2MnO_3. Only the scale factor and lattice parameters for Li_2MnO_3 were refined because of its small content (<5%). To obtain better consistency between the X-ray and neutron diffraction data, several constraints were imposed in the final refinements. The occupancy of the octahedrally-coordinated manganese ions at the 16*d* sites was finally refined using the X-ray diffraction data because manganese is more sensitive to X-rays, while the occupancy of lithium at the 8*a* sites and oxygen at the 32*e* sites, and isotropic thermal parameters, *B*, were determined using the neutron diffraction data. The final observed, calculated, and difference profiles are shown in Fig. 3, and the refined lattice parameter, atomic coordinates, and thermal parameters for $Li_4Mn_5O_{12}$ prepared at 700 °C are listed in Table 1.

The site occupancies listed in Table 1 confirmed that the distribution of cations is very close to that in the ideal arrangement, $(\mathrm{Li})_{8a}[\mathrm{Li}_{1/3}\mathrm{Mn}_{5/3}]_{16d}\mathrm{O}_4$. The occupation of the interstitial 16*c* sites by Li and the 8*a* sites by manganese are ruled out. Allowing variation of the oxygen site occupancy factor results in a value of 1.0 within the estimated standard deviation (e.s.d.), which indicates that this sample is very nearly stoichiometric with respect to oxygen. Instead, the occupancy of manganese at the 16*d* sites, $g(\mathrm{Mn})$, is found to be 0.84, with an e.s.d. of 0.02. The value of $g(\mathrm{Mn})$ is a little higher but in good agreement with 0.833 for the ideal cation arrangement of $Li_4Mn_5O_{12}$, in which 0.333 Li ions are required to compensate the imbalance in charge in the 16*d* sites assuming all the manganese ions are in the (4+) oxidation state. From an electroneutrality point of view, a higher value of $g(\mathrm{Mn})$ indicates the presence of Mn^{3+} ions.

Table 1
Structural parameters of $Li_4Mn_5O_{12}$ prepared from LiOAc and $Mn(NO_3)_2$ at 700 °C under flowing oxygen

Space group	$Fd\bar{3}m$	No. 227	a [b] = 8.1594(3) Å	a [c] = 8.1596(2) Å
Atom	site	$x=y=z$	g	B (Å^2)
Li(1)	8*a*	0.0	1.00(5) [c]	1.0(2) [c]
Li(2) [a]	16*d*	0.625	0.16	= B(Mn)
Mn	16*d*	0.625	0.84(2) [b]	0.40(5) [b]
O	32*e*	0.3878(3) [b] 0.3880(1) [c]	1.00(2) [c]	0.80(4) [c]

All numbers in the parentheses present the e.s.d. of the last significant digit, and g is the occupancy
[a] Constraints on occupancies $g(\mathrm{Mn}) + g(\mathrm{Li}(2)) = 1$ and isotropic thermal parameters $B(\mathrm{Li}(2)) = B(\mathrm{Mn})$ were applied
[b] Parameters refined using the X-ray diffraction data
[c] Parameters refined using the neutron diffraction data

3.3. Structural changes of $Li_4Mn_5O_{12}$ with synthesis temperatures

Analogous refinement of diffraction data for samples prepared at low temperature resulted in similar structural parameters. The structural parameters for the sample prepared at 500 °C are almost identical to those of the sample prepared at 700 °C, except for the lattice parameter $a = 8.1405(10)$ Å. It means about 0.7% contraction in the unit-cell volume compared with that of the sample prepared at 700 °C. The refined occupancy of manganese at the 16*d* sites, $g(\mathrm{Mn})$, is

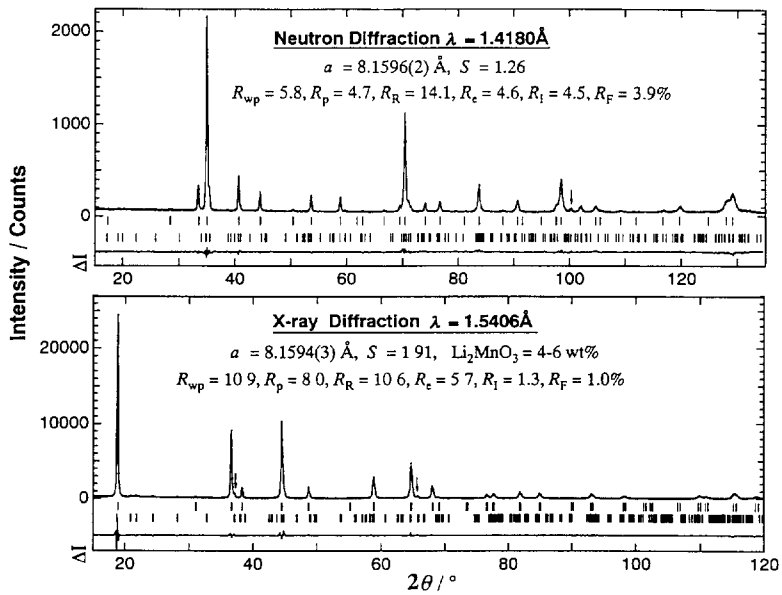

Fig. 3. Rietveld-refinement profiles for the $Li_4Mn_5O_{12}$ sample prepared at 700 °C. Observed (dots) and calculated (solid line) intensities are shown at the top, and the difference between the observed and calculated intensities (ΔI) at the bottom. The tick marks below the patterns indicate the positions of all possible Bragg reflections due to $Li_4Mn_5O_{12}$ (upper) and Li_2MnO_3 (lower). R factors as defined in Ref. [9] are given for reference.

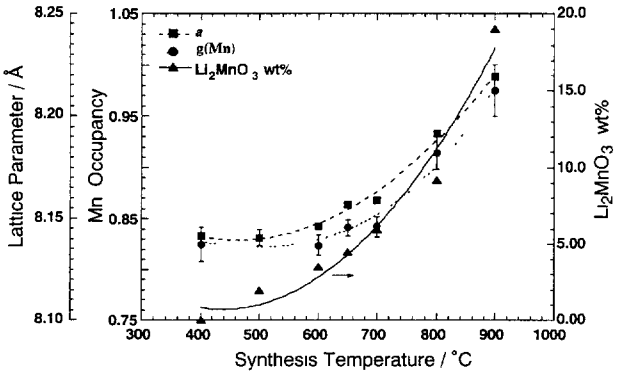

Fig. 4. Plot of the refined g(Mn), the portion of precipitated Li_2MnO_3 versus synthesis temperature, along with the lattice parameter for the spinel phase.

0.83 ± 0.01 which is identical to 0.833 for the ideal arrangement, indicating that the oxidation state of manganese in this sample is very close to (4+).

Refinement of g(Mn) revealed that g(Mn) increases with synthesis temperature. The refined occupancy, g(Mn), in the spinel phase, and the portion of precipitated Li_2MnO_3 in the final product are plotted in Fig. 4 versus the synthesis temperature, along with the lattice parameter. As the synthesis temperature was raised to 900 °C, g(Mn) reached 1.0, which indicates changes in the composition of the spinel phase. Since no evidence for oxygen deficiency at the 32e sites was found in these refinements, the spinel phase should have a composition of $Li_{1+x}Mn_{2-x}O_4$ ($1/3 \leq x \leq 0$), lying on the tie line between $Li_4Mn_5O_{12}$ and $LiMn_2O_4$ in the Li–Mn–O diagram [2,3]. The compositional change of the spinel phase from $Li_4Mn_5O_{12}$ to $LiMn_2O_4$, thus, can be expressed as

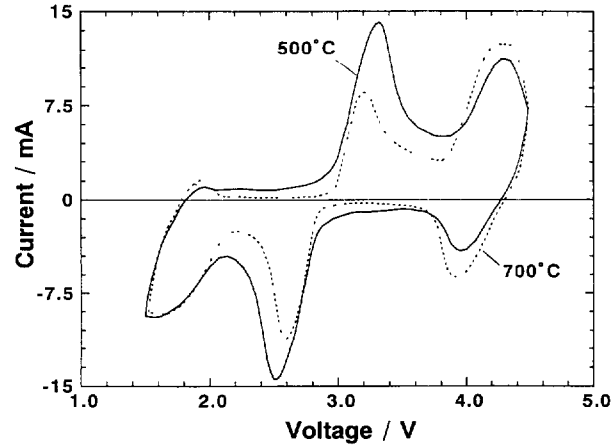

Fig. 5. Cyclic voltammograms within the 1.5–4.6 V potential range for Li/$Li_4Mn_5O_{12}$ cells using samples prepared at 500 and 700 °C, respectively.

$$Li_4Mn_5O_{12} \xrightarrow{>700\,^{\circ}C \text{ in } O_2} \alpha\, Li[Li_xMn_{2-x}]O_4 + \beta\, Li_2MnO_3 + \epsilon\, O_2\uparrow \quad (1)$$

As temperature increases, x decreases from 1/3 to 0, the lithium ions at the octahedral 16d sites are replaced by Mn^{3+} ions. Therefore, the increase in lattice parameter with synthesis temperature can be easily ascribed to the presence of larger Mn^{3+} ions in the samples prepared at elevated temperatures. The effective ion radii of octahedrally coordinated Mn^{3+} and Mn^{4+} are 0.645 (at high spin state) and 0.56 Å, respectively. The precipitation of Li_2MnO_3, thus, occurs to consume the excess lithium. Details of this compositional change was discussed separately [6].

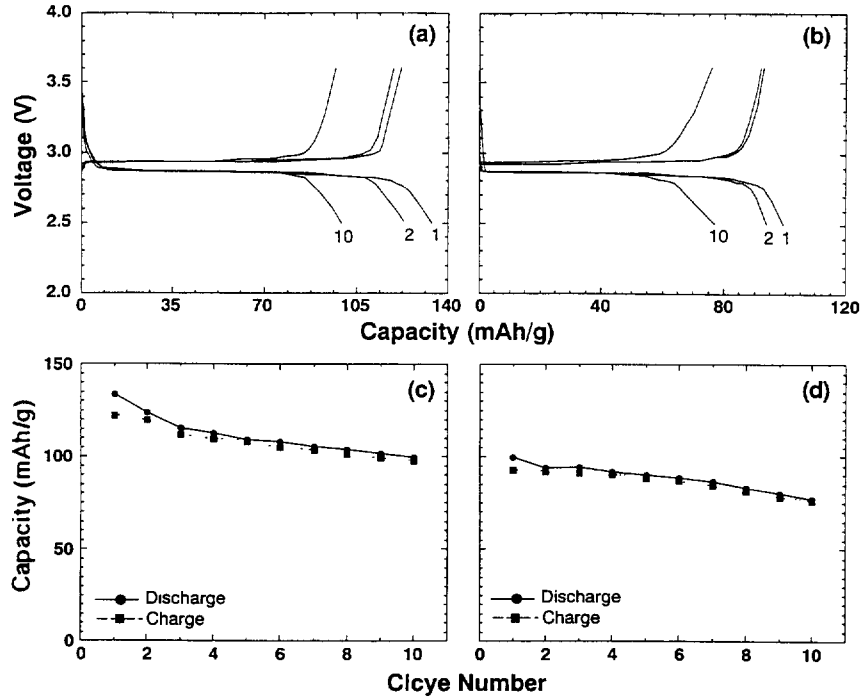

Fig. 6 Charge/discharge profiles for the initial ten cycles of Li/$Li_4Mn_5O_{12}$ cells using the powder samples synthesized at (a) 500 °C, and (b) at 700°C. The capacity delivered per cycle for these cells is shown in the corresponding figures below, (c) and (d), respectively.

3.4. Electrode performance of $Li_4Mn_5O_{12}$

The cyclic voltammograms between 1.5 and 4.6 V swept at 1.0 mV/s are shown in Fig. 5 for $Li/Li_4Mn_5O_{12}$ cells. The sample prepared at 500 °C showed a larger peak around 2.6 V but a smaller one at 3.9 V than those of the sample prepared at 700 °C. Theoretically, $Li_4Mn_5O_{12}$ offers no capacity at the 4.0 V region because manganese ions are tetravalent and it is not possible to oxidize these cations further by electrochemical extraction of lithium at practical voltages (<5.0 V). Therefore, the peak around 3.9 V indicates that the oxidation state of manganese should be less than 4.0, thus, a portion of Mn^{3+} ions exists in these samples. The larger peak at 3.9 V reveals that a larger portion of the Mn^{3+} ions is presented in the sample prepared at higher temperature. This is in good agreement with the results of Rietveld refinements.

Fig. 6 shows the initial ten charge and discharge profiles of two $Li/Li_4Mn_5O_{12}$ cells, when cycled between voltage limits of 2.5 V and 3.6 V, at a current density of 0.3 mA/cm^2, and the cycle performance given in the cathode capacity delivered per cycle, calculated for the mass of active material only. Active materials synthesized at 500 °C shown in Fig. 6(a) and (c), and 700 °C shown in Fig. 6(b) and (d), have similar charge/discharge profiles around 2.9 V. The cell using the sample synthesized at 700 °C showed a much lower capacity and a continuous decrease in capacity with cycling from 100 to 76 mAh/g after the initial ten cycles. While the cell using the sample synthesized at 500 °C had better capacity retention and delivered over 100 mAh/g after initial ten cycles. Consequently, the oxidation state of manganese in $Li_4Mn_5O_{12}$ has a profound effect on the electrode performance of $Li/Li_4Mn_5O_{12}$ cells. Synthesis of $Li_4Mn_5O_{12}$ with all manganese ions in the oxidation state of (4.0+) is the decisive factor in obtaining good electrode performance.

4. Conclusions

Well-crystallized $Li_4Mn_5O_{12}$ has been prepared from the eutectic of LiOAc and $Mn(NO_3)_2$ under flowing oxygen. Rietveld refinements with the X-ray and neutron powder diffraction data indicated that $Li_4Mn_5O_{12}$ possesses a cubic spinel structure, in which, lithium ions occupy both the tetrahedral 8*a* sites, and part of the octahedral 16*d* sites, but not the 16*c* sites, while all the manganese ions occupy the 16*d* sites. The lattice parameter was found to be sensitive to the synthesis temperature as a result of the variation in the oxidation state of manganese. The sample prepared at 500 °C showed better electrode performance: a rechargeable capacity of about 135 mAh/g for the cell $Li/Li_4Mn_5O_{12}$ in the range of cell voltages 2.5–3.6 V. It is found that the oxidation state of manganese in $Li_4Mn_5O_{12}$ has a strong effect on the electrode performance of $Li/Li_4Mn_5O_{12}$ cells.

Acknowledgements

The authors would like to thank Mr A. Goto, Dr M. Yoshikawa, Hitachi, and Dr T. Horiba, Shin-Kobe Electric Machinery, for performing the electrochemical measurements. The neutron diffraction work was conducted at Oak Ridge National Laboratory which is managed by Lockheed Martin Energy Research for the US Department of Energy under contract no. DE-AC05-96OR22464.

References

[1] J.M Tarascon, W R McKinnon, F Coowar, T.N. Bowmer, G. Amatucci and D Guyomard, *J Electrochem. Soc., 141* (1994) 1421–1431.
[2] R.J. Gummow, A. de Kock and M.M Thackeray, *Solid State Ionics, 69* (1994) 59–67.
[3] M M Thackeray, M.F. Mansuetto, D.W. Dees and D R. Vissers, *Mater. Res. Bull., 31* (1996) 133–140.
[4] T. Takada, H. Hayakawa and E. Akiba, *J. Solid State Chem., 115* (1995) 420–426.
[5] T. Takada, H Hayakawa, T Kumagai and E. Akiba, *J Solid State Chem., 121* (1996) 79–86.
[6] T Takada, H. Hayakawa, E Akiba, F Izumi and B. Chakoumakos, *J Solid State Chem.*, submitted for publication.
[7] M.N. Richard, E.W. Fuller and J R Dahn, *Solid State Ionics, 73* (1994) 81–91.
[8] F. Izumi, in R.A. Young (ed.), *The Rietveld Method*, Oxford University Press, New York, 1st edn., 1993, Ch. 13, p 236
[9] R A Young, in R.A. Young (ed.), *The Rietveld Method*, Oxford University Press Inc., New York, 1st edn., 1993, Ch. 1, p 22.
[10] P. Strobel and B. Lambert-Andron, *J. Solid State Chem., 75* (1988) 90–98.